10/1/91
E 6319

# Experimental and Analytical Analysis of Stress-Strain Behavior in a [90°/0°]$_{2s}$, SiC/Ti-15-3 Laminate

Bradley A. Lerch and Matthew E. Melis
*National Aeronautics and Space Administration*
*Lewis Research Center*
*Cleveland, Ohio*

and

Mike Tong
*Sverdrup Technology, Inc.*
*Lewis Research Center Group*
*Brook Park, Ohio*

August 1991

**NASA**

# EXPERIMENTAL AND ANALYTICAL ANALYSIS OF STRESS-STRAIN BEHAVIOR IN A [90°/0°]$_{2s}$, SiC/Ti-15-3 LAMINATE

Bradley A. Lerch and Matthew E. Melis
National Aeronautics and Space Administration
Lewis Research Center
Cleveland, Ohio 44135

and

Mike Tong
Sverdrup Technology, Inc.
Lewis Research Center Group
Brook Park, Ohio 44142

## Summary

The nonlinear stress-strain behavior of a [90°/0°]$_{2s}$, SiC/Ti-15-3 composite laminate was numerically investigated with a finite element, unit cell approach. Tensile stress-strain curves from room temperature experiments depicted three distinct regions of deformation, and these regions were predicted by finite element analyses.

The first region of behavior, which was linear elastic, occurred at low applied stresses. As applied stresses increased, fiber/matrix debonding in the 90° plies caused a break in the stress-strain curve and initiated a second linear region. In this second region, matrix plasticity developed in the 90° plies. The third region, which was typified by nonlinear, stress-strain behavior, occurred at high stresses. In this region, the onset of matrix plasticity in the 0° plies stiffened the laminate in the direction transverse to the applied load. Metallographic sections confirmed the existence of matrix plasticity in specific areas of the structure, and finite element analyses also predicted these locations of matrix slip.

## Introduction

Before composites can be modeled properly, the development of damage must be understood. The correct deformation response and fracture behavior of each constituent must be incorporated into any model that is to describe the composite behavior. Some damage, such as fiber and matrix cracking, can be documented metallographically in post-test examinations. Other damage, such as interface separation or matrix plasticity, is frequently difficult to observe. Slip, in particular, is difficult to observe in some materials. With respect to fiber and matrix debonding, the interface region is very small, and the resolution of cracks is, therefore, also a problem. However, the effect of these two damage modes on the stress-strain behavior can be considered through numerical analysis.

Nonlinear finite element analyses were performed in this study to help explain the behavior of a [90°/0°]$_{2s}$ SiC/Ti metal matrix composite undergoing tensile loading. The existence of the damage mechanisms mentioned previously was demonstrated through both experimental and numerical data. Consistency between experimental and analytical results gave credence to the capabilities of the finite element analysis.

## Material

Before the problem is described, a brief explanation of the material is warranted so that the various damage modes can be easily understood. The [90°/0°]$_{2s}$ laminates consisted of eight plies in which SiC (SCS-6) fibers were embedded within a Ti-15-3 (Ti-15V-3Cr-3Al-3Sn) matrix. The fibers, which comprised 34 vol % of the composite, were coated with a 3-$\mu$m-thick, double-pass carbon coating. This coating is weak, causing fiber/matrix debonding at low stresses (ref. 1). The outer portion of this carbon coating reacts with the matrix

upon consolidation to form a 0.3-μm-thick reaction zone. Figure 1 gives an example of the fiber, interface, and matrix; and reference 2 gives more details about the interface.

## Tensile Behavior

Several tensile tests, all producing consistent results, were conducted at room temperature in strain control. Dog-bone-shaped, 6-in. long specimens were cut from the composite plates such that the tensile load was applied parallel to the fiber axis in the 0° plies (fig. 2). Strains were measured with a clip-on extensometer and with 0°/90° strain gage rosettes. The extensometer and the 0° strain gage gave similar axial strains. Transverse strains (i.e., strains perpendicular to the loading direction) were measured with the 90° strain gage. A representative, experimental stress-strain response of the SiC/Ti specimens under tensile load is depicted in figure 3. Both the axial and transverse strains are shown as a function of the applied stress.

There are three distinct regions common to the tensile curves. The first region lies between 0 ksi and approximately 20 ksi. In this region, the stress-strain behavior is linear, but at 20 ksi, a knee occurs in both curves. This change has been associated with fiber/matrix debonding in the 90° plies due to the weak interface (ref. 1). Between approximately 20 and 80 ksi, a second linear region occurs. The third region, from 80 ksi to fracture, is characterized by nonlinear behavior, the origin of which is not clear. This third region is unique because the composite becomes stiffer in the transverse direction (effective Poisson's ratio increases) as the applied stress increases (fig. 3). This phenomenon prompted us to use finite element analysis to further investigate the material response.

# Analysis Models

Two three-dimensional, finite element meshes of the composite were generated with the help of COMGEN (ref. 3), which creates geometric and discrete composite models in a PATRAN data base. PATRAN (ref. 4), a finite element pre-processor and post-processor, translated the model data for submission to the general purpose, finite element analysis code MARC (ref. 5). The results, which were sent back to PATRAN for post-processing, are described later.

Initially, a relatively large model was created to represent the $[90°/0°]_{2s}$ fiber layup in the composite. This model (fig. 2) consisted of 4121 nodes and 3456 eight-node, hexagonal elements. (Note that the shaded regions in the model represent the fibers.) The preliminary elastic analyses of this model required large amounts of time on the CRAY YMP, suggesting that unacceptable time requirements would be needed for an iterative nonlinear analysis. Therefore, with the help of symmetric considerations, a smaller model (fig. 4) was created from the larger. This model, containing 623 nodes and 432 elements, proved to be more manageable on the computer. In addition, elastic analyses identical to those run on the larger

model were performed on the smaller model. The results proved to be consistent, providing a degree of confidence in the smaller model, so the smaller model was used for the remaining analyses in this study.

Since there were some initial concerns about the relatively coarse mesh density of the model, two additional models were made, one containing a finer meshing pattern and the second containing a higher order element (20-node brick). The results from these new models were essentially the same as those from the initial small model. Therefore, the initial model selected was considered adequate for the study.

Constraints on the model were intended to provide a generalized plane strain condition. That is, the nodes on the free faces of the model were constrained to remain planar with one another if any displacement took place. This assumption comes from classical laminate plate theory, which states that shearing deformations in the structure are neglected, thus plane sections remain plane. It is possible that the interface between the fiber and the matrix might allow movement between the two constituents, which would invalidate the plane strain assumption. However, since little is known about the mechanical properties of the interface, we deemed it impractical to model the interface directly with finite elements. Therefore, we adopted the plane strain assumption.

Previous investigations of the composite suggested that fiber/matrix debonding occurred under tensile loading (ref. 1). To account for this numerically, we placed gap elements between the fiber and matrix elements such that the two would separate under radial tension. Although this was not the ideal way to model the interface, we assumed it to be adequate for this study.

During the cooldown portion of the composite fabrication process, significant residual stresses developed because of the thermal coefficient of expansion mismatch between the fiber and the matrix. Hence, loads imposed on the model were both thermal and mechanical. These residual stresses could be predicted when the model was "cooled" from 1300 to 70 °F. The high end of this range represents the heat treatment temperature and the assumed stress-free state of the material during its fabrication process.

The mechanical loads imposed on the model were uniform pressure loads that were perpendicular to one of the Y-Z faces in figure 4. These loads were increased incrementally until the experimental ultimate tensile strength was reached. Our intent was only to simulate uniaxial tension in the material. The other Y-Z face of the model had its nodes constrained to remain in that plane to prevent rigid body motion. Strains were calculated from the displacements of the entire model and not of individual elements.

Material properties used for this model were both elastic and inelastic. The matrix, which was elastic-plastic, was described from experimentally measured stress-strain curves (ref. 6) in the piecewise linear fashion typically used for nonlinear finite element analysis (ref. 5). In addition, the temperature dependence of the material was accounted for through the input of experimental curves for several different

temperatures. Because the fiber is ceramic, it was treated as elastic throughout the analyses. Final data reduction from the analyses characterized the global response of the finite element model. From this, the experimental stress-strain response of the material could be directly compared with the analyses. These results are outlined and discussed in the following section.

## Nonlinear Finite Element Analysis

The numerical model and the boundary conditions just described were used for elastic-plastic structural analyses of the behavior of the composite laminate. Three cases were studied:

(1) Temperature cooldown from 1300 to 70 °F followed by tensile load; perfect bonding assumed between fiber and matrix (no gap elements)

(2) Tensile load only (no residual stresses from cooldown); gap elements included to simulate any debonding at the fiber/matrix interface

(3) Temperature cooldown from 1300 to 70 °F followed by tensile load; gap elements included to simulate any debonding at the fiber/matrix interface as a result of cooldown or load application

## Results

With the perfect bonding assumption (case 1), the finite element method predicted the initial linear portion at lower stresses (figs. 5 and 6), particularly in the axial direction. However, since the knee in the curve (signifying the change to the next region) was not captured, both predicted curves remained linear up to very high stresses, unlike the experimental results.

With the gap elements simulating debonding at the fiber/matrix interface, but without including residual stresses (case 2), the finite element method again failed to predict the proper stress-strain behavior. No bilinear stress-strain behavior was predicted at low stresses (figs. 7 and 8). In addition, the slope of the linear portion of the curve was lower than the initial experimental elastic modulus and was, in fact, equal to that of the second linear region. This result indicates that debonding has already occurred. Examination of the gap elements showed that the gaps opened immediately upon loading since there were no compressive residual stresses to keep them closed. Under these loading conditions, the finite element model predicted some nonlinearity at high applied stresses in the axial direction, but it did not predict the stiffening of the laminate in the direction transverse to the load as indicated in the experiment.

Because the residual stresses from the temperature cooldown in the laminate were accounted for and gap elements were used (case 3), the stress-axial strain behavior did agree reasonably

well with the experimental results. However, the stress-transverse strain behavior predicted by the finite element analysis slightly underestimated the experimental data. The analysis predicted that the knee in both stress-strain curves would occur at approximately 20 ksi (figs. 9 and 10). In addition, it predicted some stiffening in the direction transverse to the load at high applied stresses, as also indicated by the experiment (fig. 10).

With these final loading conditions (case 3), the development of damage within the composite can be followed. At an applied stress of 20 ksi, the gap elements at location "A" in the 90° plies (fig. 4) begin to open. In fact, Johnson et al. observed this behavior (ref. 1) through edge replication techniques. They found that the interface begins to debond at ~20 ksi for 0°/90° orientations and in the locations indicated in the present analysis. This gap opens when the applied local tensile stresses are equal to the residual, radial compressive stresses. This relationship, which has also been suggested by others (refs. 1 and 7), indicates that the fiber/matrix interface has, for all practical purposes, no strength. In other words, in the pretested state, the fibers are not bonded to the matrix and are held in place primarily by the residual stresses. The opening of these gap elements roughly coincides with the "knee" that appears at approximately 20 ksi in the stress-transverse strain and stress-axial strain experimental curves (fig. 3). This knee marks the end of the first region in the stress-strain behavior.

Up to an applied stress of 40 ksi, the matrix remained elastic. Equivalent plastic strain (based on the Von Mises yield criterion) was predicted at 40 ksi (fig. 11) in the 90° plies at location "B" (fig. 4), 90° from the opened gap elements. The predicted size of this plastic zone increases with increasing load. The continued interfacial debonding and the growth of the plastic zone in the 90° plies is typified by the second linear region of the stress-strain curve.

At an applied stress of 70 ksi, the matrix in the 0° plies began to flow plastically (fig. 12). This development occurred concomitantly with the upward turn in the transverse strain (fig. 10), as well as with the nonlinear behavior in the stress-axial strain curve (fig. 9).

One final point of interest can be observed in figures 13 to 15, in which predicted areas and concentrations of matrix plasticity (fig. 13) can be compared with those observed experimentally (figs. 14 and 15). A post-test heat treatment (ref. 8) revealed slip bands in the matrix of the deformed specimens. As shown in reference 8, slip bands result from tensile deformation - not from composite consolidation.

Figures 14 and 15 show metallographic sections of both the X-Y face (transverse to the 90° plies) and the Y-Z face (transverse to the 0° plies), respectively, after the test was interrupted at 120 ksi. As evidenced by the high density of the slip bands, plastic deformation is concentrated at area "B" in the 90° plies (fig. 14). The dashed lines in the micrograph demarcate the areas of slipped and nonslipped matrix and show a triangular shape between fibers as predicted by the

3

finite element analysis. The Y-Z face (fig. 15) shows a more wavy slip between the 0° and 90° plies, similar to the predicted pattern. These results imply two things: first that the agreement between the experimental and numerical data suggests valid results from both and, more importantly, that the finite element method can accurately assess composite material behavior at both the micro and macro levels.

## Summary and Conclusions

The nonlinear stress-strain behavior of a $[90°/0°]_{2s}$, SiC/Ti-15-3 composite was investigated with a finite element unit cell approach. Stress-strain curves, derived from tensile tests at room temperature, exhibited three distinct regions of behavior. At low applied stresses, the composite remained elastic, and the stress-strain curves were linear. Between 20 and 70 ksi, a second linear region occurred, which was found to result from debonding and matrix plasticity in the 90° plies. The third region occurred at higher stresses. In this region, nonlinear behavior in the stress-axial strain curve and stiffening in the stress-transverse strain curve resulted from matrix plasticity in the 0° plies. Metallography confirmed the existence of matrix plasticity in specific areas of the composite as predicted by the finite element analysis.

## References

1. Johnson, W.S.; Lubowinski, S.J.; and Highsmith, A.L.: Mechanical Characterization of Unnotched SCS6/Ti-15-3 Metal Matrix Composites at Room Temperature. Thermal and Mechanical Behavior of Metal Matrix and Ceramic Matrix Composites, J.M. Kennedy, H. Moeller, and W.S. Johnson, eds., ASTM STP-1080, 1990, pp. 193-218.

2. Lerch, B.A.; Hull, D.R.; and Leonhardt, T.A.: Microstructure of a SiC/Ti-15-3 Composite. Composites, vol. 21, no. 3, May, 1990, pp. 216-224.

3. Melis, M.E.: COMGEN: A Computer Code for Generating Finite Element Models of Composite Materials at the Micro Level. NASA TM-102556, 1990.

4. PATRAN II Users Manual. PDA Engineering, Santa Ana, CA, 1984.

5. MARC General Purpose Finite Element Program. MARC Analysis Research Corporation, Palo Alto, CA, 1983.

6. Lerch, B.A.; Gabb, T.P.; and MacKay, R.A.: Heat Treatment Study of the SiC/Ti-15-3 Composite System. NASA TP-2970, 1990.

7. Nimmer, R.P.: Fiber-Matrix Interface Effects in the Presence of Thermally Induced Residual Stresses. J. Compos. Technol. Res., vol. 12, no. 2, Summer, 1990, pp. 65-75.

8. Lerch, B.A.: Matrix Plasticity in SiC/Ti-15-3 Composite. NASA TM-103760, 1991.
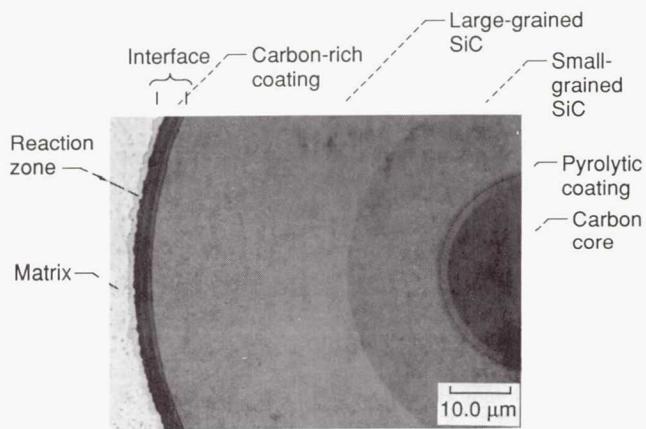
Figure 1.—Portion of the interface region showing the weak carbon coating.
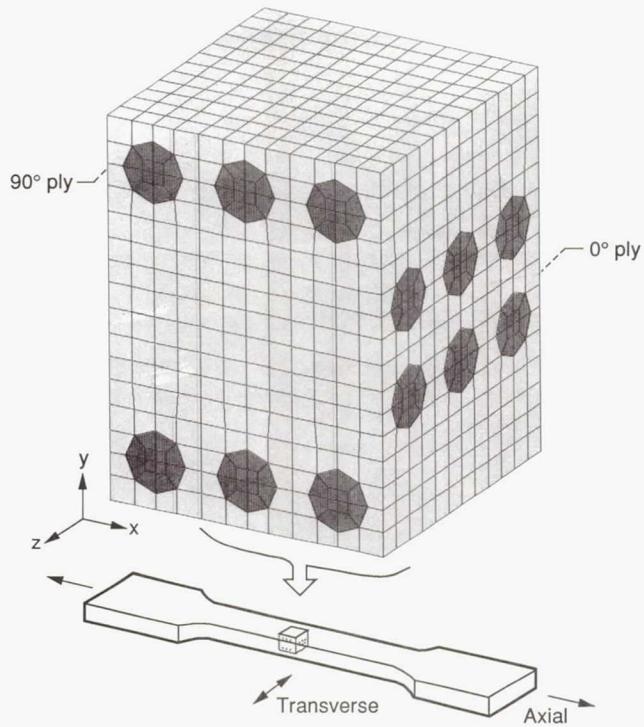


Figure 2.—Large finite element model of [90°/0°]$_{2s}$ laminate. Tensile specimen indicates the relationship between the loading axis and the 0° and 90° plies.
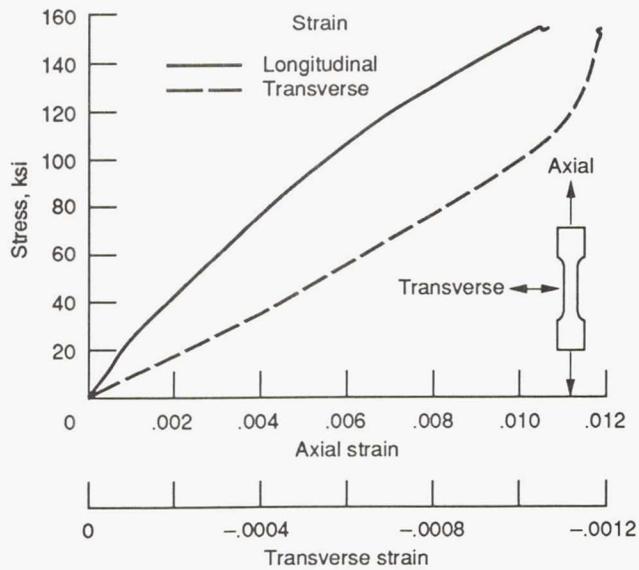


Figure 3.—Experimental stress-strain curves in both axial and transverse directions.
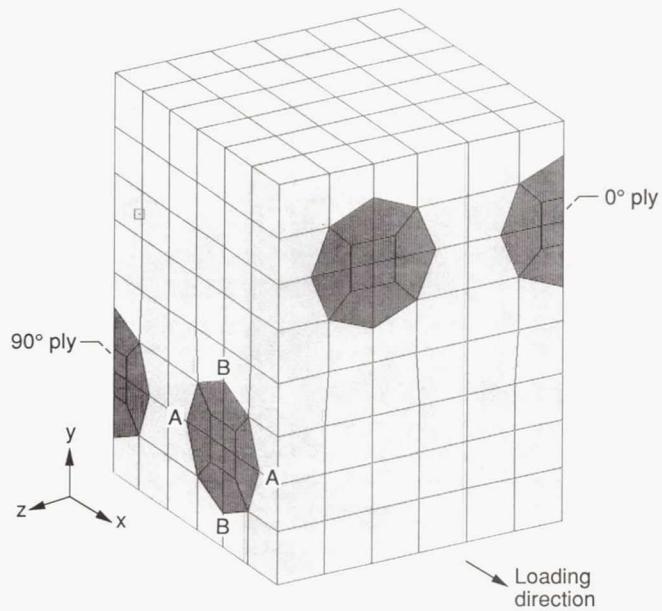


Figure 4.—Small finite element model. Area "A" debonds during tensile loading, whereas area "B" shows concentrations of matrix plasticity.
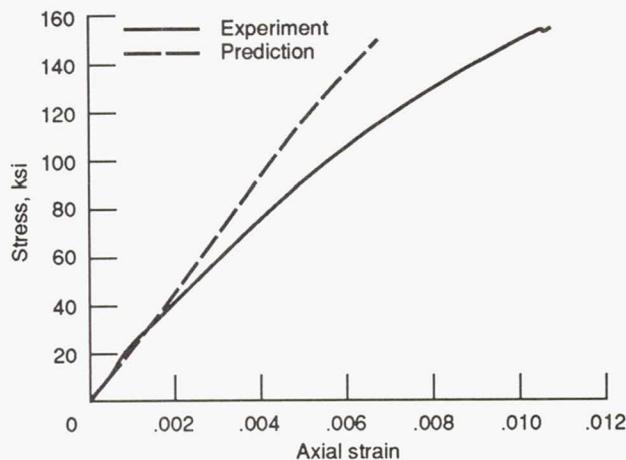
Figure 5.—Stress-axial strain curves. Predicted curve was modeled for conditions of cooldown and perfect interfacial bond.
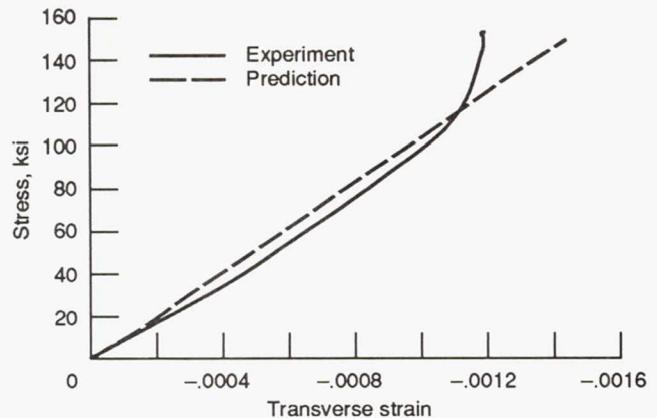


Figure 6.—Stress-transverse strain curves. Predicted curve was modeled for conditions of cooldown and perfect interfacial bond.
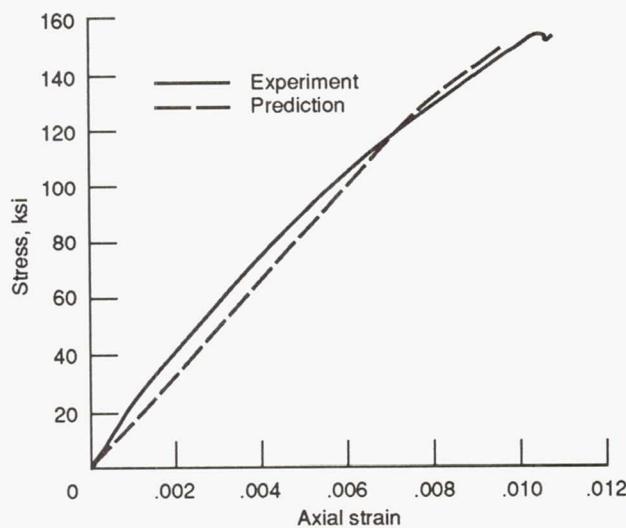


Figure 7.—Stress-axial strain curves modeled with interfacial gap elements included (no cooldown).
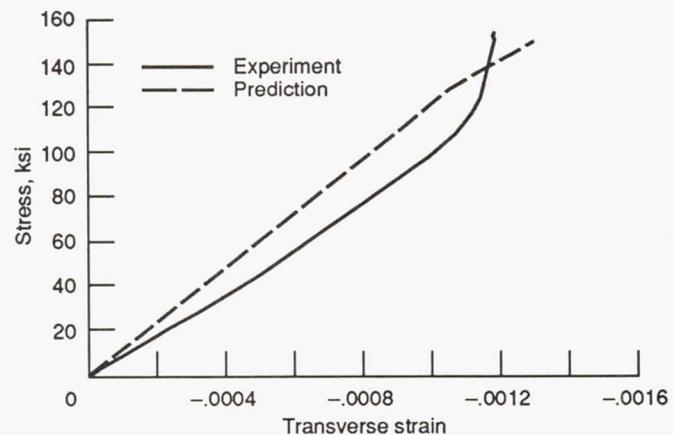


Figure 8.—Stress-transverse strain curves modeled with interfacial gap elements included (no cooldown).
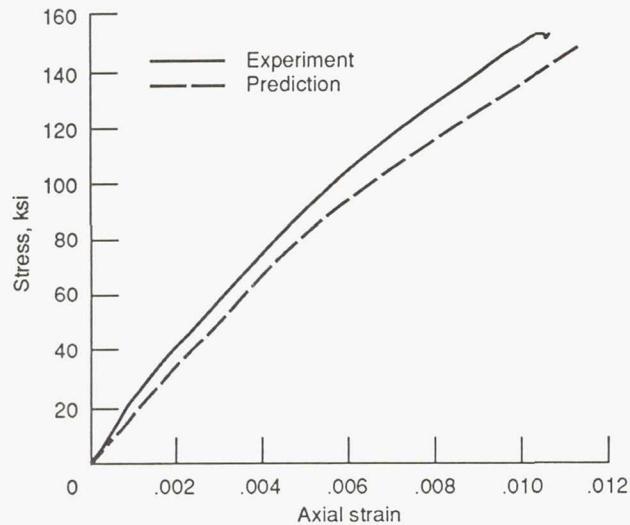
Figure 9.—Stress-axial strain curves modeled with interfacial gap elements and cooldown included.
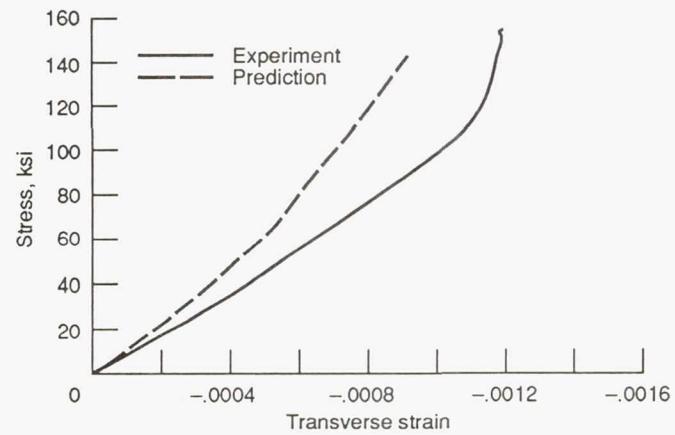


Figure 10.—Stress-transverse strain curves modeled with interfacial gap elements and cooldown included.
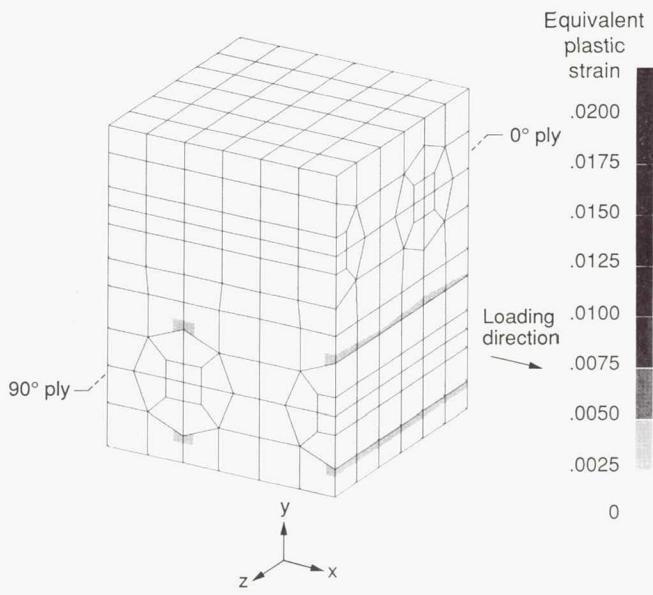


Figure 11.—Predicted extent of matrix plasticity after loading to 40 ksi.
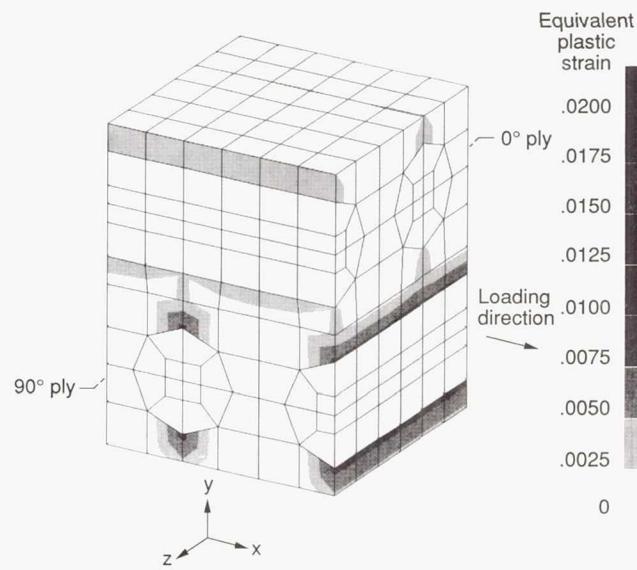


Figure 12.—Predicted extent of matrix plasticity after loading to 70 ksi.

7
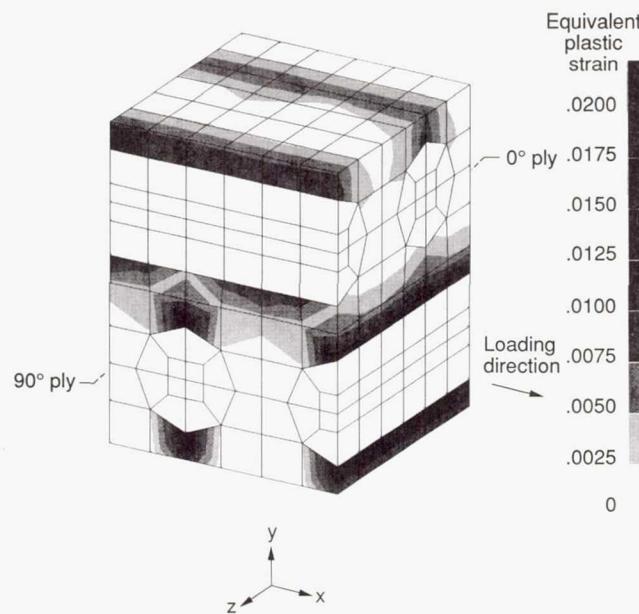
Figure 13.—Predicted extent of matrix plasticity after loading to 120 ksi.



(a) Matrix plasticity predicted from finite element analysis.

(b) Slip bands observed in metallographic section.
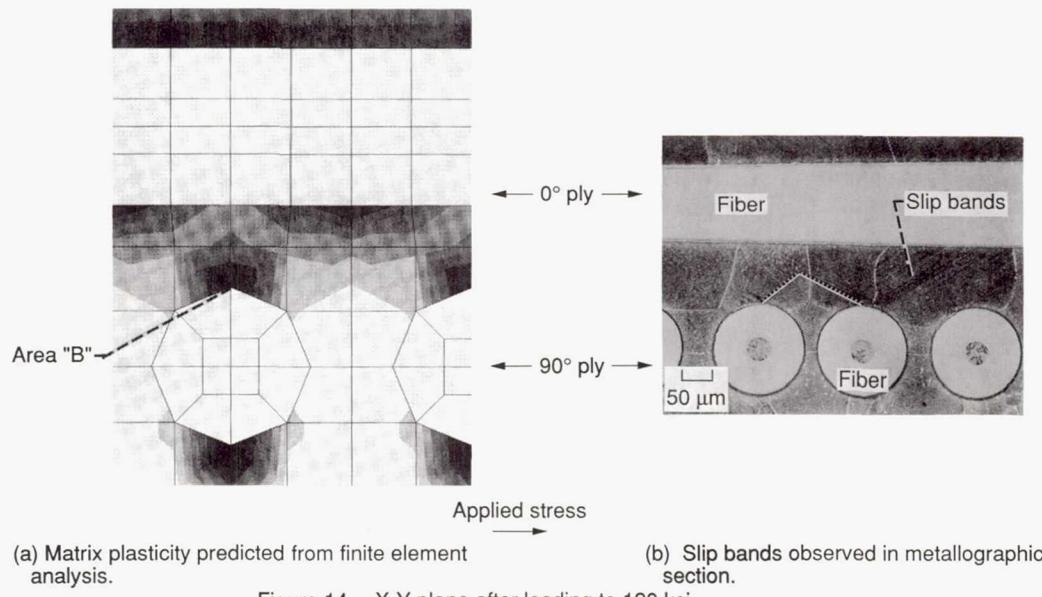
Figure 14.—X-Y plane after loading to 120 ksi.
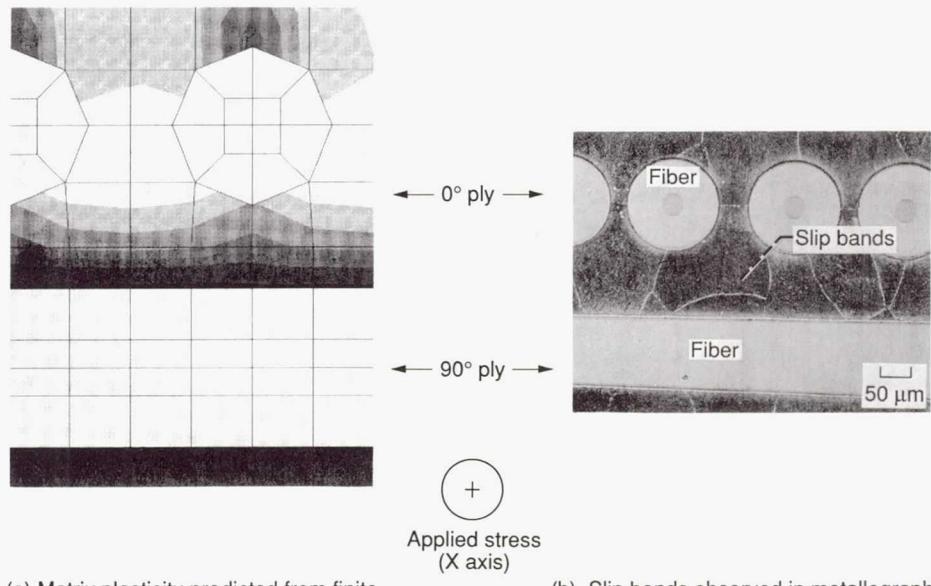
8

←— 0° ply —→

←— 90° ply —→

⊕

Applied stress
(X axis)

(a) Matrix plasticity predicted from finite
element analysis.

(b) Slip bands observed in metallographic
section.

Figure 15.—Y-Z plane after loading to 120 ksi.

**16. Abstract**

The nonlinear stress-strain behavior of a $[90°/0°]_{2s}$, SiC/Ti-15-3 composite laminate was numerically investigated with a finite element, unit cell approach. Tensile stress-strain curves from room temperature experiments depicted three distinct regions of deformation, and these regions were predicted by finite element analyses. The first region of behavior, which was linear elastic, occurred at low applied stresses. As applied stresses increased, fiber/matrix debonding in the 90° plies caused a break in the stress-strain curve and initiated a second linear region. In this second region, matrix plasticity in the 90° plies developed. The third region, which was typified by nonlinear, stress-strain behavior occurred at high stresses. In this region, the onset of matrix plasticity in the 0° plies stiffened the laminate in the direction transverse to the applied load. Metallographic sections confirmed the existence of matrix plasticity in specific areas of the structure, finite element analyses also predicted these locations of matrix slip.

| 17. Key Words (Suggested by Author(s))<br>Metal matrix composites; Tensile tests; Tensile deformation; Finite element method | 18. Distribution Statement<br>Unclassified - Unlimited<br>Subject Category 24 |
|---|---|

| 19. Security Classif. (of the report)<br>Unclassified | 20. Security Classif. (of this page)<br>Unclassified | 21. No. of pages<br>10 | 22. Price*<br>A02 |
|---|---|---|---|